J Food Sci Technol (September 2019) 56(9):4349–4358
https://doi.org/10.1007/s13197-019-03903-6

ORIGINAL ARTICLE

Synthesis of catalyst composed of palygorskita-TiO_2 and silver nanoparticles for the development of assays antioxidant based on the generation of reactive oxygen species

Anallyne Nayara Carvalho Oliveira Cambrussi[1] · Joziel Alves De Oliveira[1] · Marcel Leiner de Sá[1] · Luis Rodrigues de Sena Neto[1] · Carla Eiras[1] · Josy Anteveli Osajima[1] · Alessandra Braga Ribeiro[1]

Revised: 19 January 2019 / Accepted: 24 June 2019 / Published online: 1 July 2019

Abstract The great interest in compounds that present antioxidant capacity has generating the urgent need for analytical methods that could determine the antioxidant potential of these sources. A method based on generation of reactive oxygen species in water from catalyst composed of palygorskita-TiO_2 and silver nanoparticles (AgNPs/TiO_2-PAL) was developed and applied to antioxidant assays. Silver nanoparticles were synthesized using silver nitrate solution, sodium borohydride reducing agent and Caraia gum as stabilizing agent. Incorporation of AgNPs into the previously synthesized TiO_2-PAL was performed. The catalyst AgNPs/TiO_2-PAL was characterized by UV–vis spectroscopy, X-ray diffractometry and scanning electron microscopy. The catalyst AgNPs/TiO_2-PAL were used to perform an antioxidant activity method which consisted in monitoring the discoloration of acid yellow 73 dye (AY73) in the presence of gallic acid antioxidant comparing to the dye discoloration in the absence of the antioxidant. A microplate reader was used to measure the discoloration of the aqueous solutions of AY73, irradiated by UV light for 60 min. The effect of reactive oxygen species generated by AgNPs/TiO_2-PAL based in photocatalytic kinetics of AY73 dye was investigated. The oxidation of AY73 dye by photocatalysis in the system with AgNPs/TiO_2-PAL catalysts was carried out mainly by the participation of $O_2^{\cdot-}$, $HO^{\cdot}$ and $^1O_2$ species, in this order of importance. The results showed that the synthesis of the AgNPs/TiO_2-PAL catalyst was successfully carried out and the application of this material in the development of an innovative methodology for the determination of antioxidant activity was extremely promising.

Keywords Palygorskite · Silver nanoparticles · TiO_2 · ROS · Antioxidant activity

✉ Alessandra Braga Ribeiro
alessandra.bragaribeiro@gmail.com

Anallyne Nayara Carvalho Oliveira Cambrussi
anallynecambrussi@gmail.com

Joziel Alves De Oliveira
jozielmateriais@gmail.com

Marcel Leiner de Sá
marcel-pi@hotmail.com

Luis Rodrigues de Sena Neto
luis.sena.ufpi@gmail.com

Carla Eiras
carla.eiras.ufpi@gmail.com

Josy Anteveli Osajima
josy_osajima@cnpq.pq.br

[1] Interdisciplinary Laboratory for Advanced Materials - LIMAV, UFPI, Teresina, PI 64049-550, Brazil

Introduction

Oxidative metabolisms are the major suppliers of energy in biological systems and are essential for the survival of cells (Rui-Jie et al. 2016). However, during these metabolic processes, reactive oxygen species (ROS) are generated, and when excess ROS overwhelms the endogenous antioxidants (superoxide dismutase, catalase, peroxidase, glutathione, vitamin C and vitamin E) damage to biological systems occurs and oxidation of compounds resulting in uncountable products, generating potential deterioration (Erel 2004; Niki 2010). Therefore, the antioxidant compounds achieved prominence within the food, cosmetic and pharmaceutical industries due to the potential to neutralize reactive species, controlling the effects of deterioration or

even physiological unbalance in the human body (Kumar et al. 2017).

The great interest in compounds/materials that present antioxidant capacity has generating the urgent need for analytical methods that could effectively determine the antioxidant potential of these sources (Ge et al. 2018). However, there is not yet a fully effective method for assessing antioxidant capacity, and disadvantages are often reported in most assays, such as high cost, extensive reagent consumption, necessity of sophisticated instruments, complexity, high reaction time, use of fluorometers, which may not be routinely available in analytical laboratories (Erel 2004; Niki 2010). It is important to highlight the fact that most commonly used methods ($ABTS^{\cdot+}$ e DPPH) are based on a large non-biological and sterically hindered radical, making difficult for antioxidants to reach the center of the radical, snot reflecting in vivo conditions (López-Alarcón and Denicola 2013).

Biologically, $HO^{\cdot}$ radicals are generated when H_2O_2 reacts with Fe(II) (Fenton type reaction). However, the use of Fenton reactions in the development of antioxidant assays has disadvantages, since many antioxidants are also metal chelators that alter Fe(II) activity after chelation (Rui-Jie et al. 2016). In this context, the heterogeneous photocatalysis of water by titanium oxide (TiO_2) nanoparticles could be used to generate reactive oxygen species for antioxidants assays (Chen et al. 2014).

A general process of photocatalysis initiates from the photoexcitation of TiO_2 with an energy greater than its band gap (Eg) of 3.2 eV (Wei et al. 2017), resulting in the formation of active electron–hole pairs (e^-/h^+) (Wei et al. 2017). In the presence of electron donors and acceptors in solution, the recombination reaction between the electron and the hole can be avoided by redox reactions. In the photolysis of TiO_2 in water, the solvating nanoparticles of the water molecules and the dissolved O_2 can react with both, the hole and the electron, respectively, to generate $HO^{\cdot}$ (Rui-Jie et al. 2016; Nagarajan et al. 2017). However, TiO_2 absorbs in a region of the spectrum, less than 380 nm, presenting low quantum yield (Chen et al. 2014). An alternative to improve the absorption profile and optimize the photodegradation process is the incorporation of metallic nanoparticles (MeNPs) to its structure (Lee and Chen 2014), since MeNPs deposited in the TiO_2 acts as an electron scavenger, decreasing the rate of recombination of electron pair/hole (e^-/h^+), improving, consequently, the photocatalytic activity of TiO_2 (Hidalgo et al. 2010).

However, despite the optimization, there are still problems regarding the removal of this catalyst from the water. TiO_2 powders have large surface areas and good catalytic activities. However, powders readily agglomerate into larger particles, resulting in an adverse effect on catalyst performance. In addition, it is very difficult to recover pure TiO_2 powders from the water when they are used in aqueous systems (Chen et al. 2014). In order to solve this problem, it is suggested the use of porous materials to support the catalyst, namely clays such palygorskite (PAL), which could increase the surface contact area and consequently facilitating the removal of the catalyst material (Verma et al. 2014). Palygorskite (PAL) is a widely used species of hydrated magnesium aluminum silicate with an elongated microfibrous morphology, had reactive groups on its surface. PAL's microscopic structure is needlelike or rod-shaped with 20–70 nm in diameter and about 1 μm in length (Ma et al. 2017). Due to its unique structure and high surface area, PAL appears as an attractive support for the immobilization of catalysts in the removal of pollutants (Chen et al. 2014).

In this context, combining PAL to support the catalyst and modification by noble metal, this work prepared a catalyst composed of TiO_2, silver nanoparticles and supported in the argilomineral palygrskite (AgNPs/TiO_2-PAL), with the objective of to develop a colorimetric method, automated in microplates, for the determination of antioxidant activity, based on the generation of reactive oxygen radical species ($HO^{\cdot}$, $O_2^{\cdot-}$, $^1O_2$), present biologically in vivo systems, using a heterogeneous photocatalysis system.

Materials and methods

Material

The P25 Degussa titanium dioxide catalyst (TiO_2) with a high purity (99.99%), was used as a comparison parameter with the results of catalyst AgNPs/TiO_2-PAL, gum Caraia, silver nitrate ($AgNO_3$), ultrapure water (MilliQ® system), sodium borohydride ($NaBH_4$), methanol, diphenylamine ($\geq$ 99%) and furfuryl alcohol (98%) were purchased from Sigma Aldrich. The EDTA disodium salt (P.A) was acquired from Dynamics Química Contemporânea LTDA. The acid yellow 73 dye (AY73), Fig. 1a, was supplied by Danny Color Dyes, and was used without prior purification. The pure anhydrous gallic acid (99.53%) was acquired in Scientific Exodus, as can be seen in Fig. 1b.

Palygorskite (PAL) was collected from the city of Guadalupe (Coimbra Company), in the State of Piauí-Brazil (06°47′13″S; 43°34′08″N). The reagents used for the synthesis of TiO_2 supported on palygorskite were titanium isopropoxide IV ($C_{12}H_{28}O_4Ti$) analytical grade 97%, hydrogen peroxide 130 vol. (35%—H_2O_2, anhydrous) and ethyl alcohol, purchased from Sigma Aldrich. The water used in all reactions was treated using the Milli-Q system.

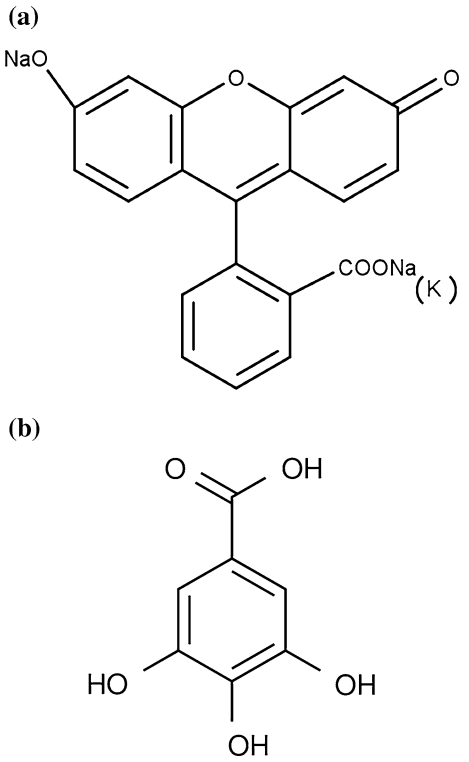

Fig. 1 Chemical structure: **a** acid yellow 73 dye and **b** gallic acid antioxidant

Synthesis of TiO_2 supported on palygorskite

Initially, the PAL was macerated and screened in a 200 mesh (74 μm), to obtain a thin powder (Zhang et al. 2011). For removal of the organic matter, the clay was washed with distilled water and then treated by hydrogen peroxide at room temperature (25 °C) for a period of 24 h. The excess of peroxide in the PAL was removed by successive washes with distilled water, followed by centrifugation. The precipitate obtained was dried at 80 °C for 12 h (Soberanis-Monforte, Gordillo-Rubio and González-Chi 2015).

For the synthesis of the TiO_2-PAL, the clay was mixed with ethanol in a ratio of 1:4 (w/v), to obtain a colloidal suspension. The mixture was kept under continuous stirring for 30 min. Simultaneously, the suspension of TiO_2 was obtained by slowly adding the precursor titanium tetraisopropoxide IV on ethyl alcohol with a ratio of 1:1.67 (w/v), with continuous stirring. After 30 min, distilled water was slowly added to the mixture in a ratio of 1:1 (v/v) to the precursor, stirring for 30 min. Subsequently the suspension of TiO_2 was added to the clay slurry and kept stirring for 30 min. The molar ratio used was 4 mmol of Ti/g of clay. After complete homogenization, the mixture was allowed to stand for 24 h. The precipitate was dried in an oven at 75 °C for 12 h. The heat treatment of the was conducted at 400 °C, on a ramp of 120 min and a heating rate of 10 °C min^{-1} (Zhang et al. 2011; Ma et al. 2017).

Synthesis of silver nanoparticles (AgNPs)

A solution of Caraia gum (1 g L^{-1}), $AgNO_3$ solution (1 mmol L^{-1}) and a solution of the reducing agent $NaBH_4$ at 1 mol L^{-1} were prepared. After preparation of solutions, a mixture of 20 mL of the $AgNO_3$ solution and 20 mL of the stabilizer solution was stirred for 1 h, then 200 μL of the $NaBH_4$ solution was added, the system was left under stirring for further 30 min.

The nanoparticles obtained were characterized using the Zetasizer Nano ZS equipment (Malvern Instruments Ltd), with a He–Ne laser of wavelength 633 nm at a temperature of 25 °C and a 90° spreading angle of on the analyzes of Dynamic Light Scattering (DLS) and Zeta Potential (PZ).

Catalyst composed of palygorskita-TiO_2 and silver nanoparticles (AgNPs/TiO_2-PAL)

A mass of the TiO_2-PAL (1.5 g) was added in 20 mL of AgNPs solution, and the system, was kept in stirring for 72 h, after the system was centrifuged, the precipitate was separated and dried in an oven for 24 h at 60 °C, followed by maceration until powder, and thus, the AgNPs/TiO_2-PAL was obtained.

AgNPs/TiO_2-PAL characterization

AgNPs/TiO_2-PAL catalyst was characterized by X-ray Diffraction (XRD) in the Shimadzu Labx-XRD 600 equipment, with Cu-Kα radiation (λ = 1.5406 Å), 2θ in the interval between 5° and 75°, with a scanning rate of 2°/min.

Scanning Electron Microscopy (SEM) with emission cannon per field in the FEI equipment, model Quanta FEG 250, with acceleration voltage of 1–30 kV, equipped with EDS of SDD (Silicon drift detectors), brand Ametek, model HX-1001, Apollo X-SDD detector. To perform the micrographs, the sample was dispersed in isopropyl alcohol, taken to the ultrasound bath for 5 min and dripped onto stub coated with foil. The drying time was around 2 h. The sample was covered with gold in the metallizer, brand Quorum, model Q150R, with time of 20 s and current of 15 mA, and plasma generated in argon atmosphere. The mean diameter of the spherical nanoparticles of the catalyst was evaluated from a 100 point measurement histogram using the ImageJ program.

To perform the EDS experiment, the sample was fixed on double-sided carbon-conductive adhesive tape and then also coated with gold. X-ray profiles were obtained at 30 kV and spot size 4.5. The presence of carbon and gold is

due to the conductive tape and metallization process, respectively.

Antioxidant capacity assays

For the tests of determination of the antioxidant capacity, chamber of radiation, provide with a 125 W without bulb. In eppendorfs, 1 mg mL^{-1} of catalyst (AgNPs/TiO_2-PAL) were mixed with 0.5 mL of aqueous solution of the AY73 in concentration 2×10^{-5} mol L^{-1} and 0.5 mL of aqueous solution of gallic acid antioxidant at varying concentrations (10–100 µg mL^{-1}), the samples were subjected to UV radiation for 60 min. After the radiation time, eppendorfs were centrifuged for 15 min at 10,000 rpm for removal of the catalyst. Thereafter, the supernatant was transferred to a microplate and the absorbance readings were performed on the microplate reader (Elisa Polaris®) at a wavelength of 492 nm and compared the absorbance readings of these same non-irradiated solutions for the calculation of the AY73 discoloration as a function of antioxidant concentration.

The discoloration of the solutions was determined using Eq. (1) (Mecha et al. 2016):

$$Discoloration\ (\%) = \frac{A_0 - A_t}{A_0} * 100 = \frac{C_0 - C_t}{C_0} * 100 \quad (1)$$

where A_0 is the initial absorbance of the solution and A_t the absorbance at time t, which relate respectively to the initial concentrations (C_o) and time t (C_t) according to the Lambert–Beer law (Tian et al. 2012). Considering the values obtained, reaction curves were created to achieve the inhibitory concentration, in vitro, to decrease in 50% the AY73 discoloration (IC_{50}) using the standard antioxidant gallic acid. Linearity was established by the standard curve for gallic acid, which was obtained in five different concentration levels. Each concentration was determined in triplicate (n = 15). The linearity was evaluated using linear regression analysis, with adjustment of the data by least squares method.

The results obtained with the method developed using the AgNPs/TiO_2-PAL catalyst was compared to the results obtained using the commercial catalyst TiO_2 P25 Degussa.

The remaining concentration of AY73 dye in solution was analyzed by UV–vis spectrophotometer (Agilent Technologies spectrophotometer, Cary 60 UV) at its maximum wavelength of 490 nm.

Scavenger study

An estimate of the contribution of hydroxyl radicals $HO^{\cdot}$, superoxide anion $O_2^{\cdot-}$, oxygen singlet $^1O_2$, and positive holes (h^+) during the assays antioxidant, are determined by adding different ROS scavenger such as methanol, diphenylamine, furfuryl alcohol and EDTA disodium salt, $HO^{\cdot}$ removers (Li and Hu 2016), $O_2^{\cdot-}$ (Alrobayi et al. 2015), $^1O_2$ (Li and Hu 2016) and h^+ (Alrobayi et al. 2015), respectively. All compounds were used at 0.5 mmol L^{-1} (Alrobayi et al. 2015).

Results and discussion

AgNPs characterization

The electrostatic stabilization of AgNPs was estimated by measuring their zeta potential values. The zeta potential value was found to be − 33.5 mV for particles, the high negative value confirms a repulsion between the particles and a good stability of the silver nanoparticles. (Agnihotri et al. 2014). DLS analysis showed the size distribution of particles with maximum intensity at 52.12 nm, which are considered as satisfactory parameters (Abou El-Nour et al. 2010).

AgNPs/TiO_2-PAL catalyst characterization

The structure of the synthesized AgNPs/TiO_2-PAL catalyst was analyzed by XRD measurements. Figure 2a shows the TiO_2 P25 Degussa diffractograms with the anatase crystallographic phase, Palygorskite clay (PAL) and AgNPs/TiO_2-PAL catalyst. The characteristic reflections of palygorskite were observed in the XRD patterns, the reflections at $2\theta = 8.34°$ and 19.7° corresponded to palygorskite (Zhang et al. 2011; Ma et al. 2017). The diffraction peaks of the AgNPs/TiO_2-PAL catalyst at $2\theta = 25.52°$, 38.78°, 48.09° correspond to the same peaks found in TiO_2 P25 Degussa diffractogram (Santana and Zaia 2006) indicating TiO_2 was crystallized in the anatase phase over the palygorskite, which presents greater photocatalytic activity (Samya et al. 2014). The addition of Ag did not change the TiO_2 profile, inferring that Ag was not dissolved in the structure of TiO_2 and, probably was deposited on its surface (Lee and Chen 2014). Some typical peaks characteristic of silver nanoparticlesare overlapped with the peaks corresponding to TiO_2, however, an EDS analysis confirms a presence of silver in the synthesized catalyst, as shown in Fig. 2b.

The SEM images (Fig. 3) revealed that these materials consisted of spherical nanoparticles with an average diameter around 1 µm, the mean diameter of the spherical nanoparticles of the catalyst was evaluated from a histogram with a measurement of 100 points, the minimum value found was 0.7818 µm and the maximum value was 2.8546 µm, it was observed that the spherical particles were formed by the aggregation of smaller particles, it can be seen fibers in planar structures, which was a typical

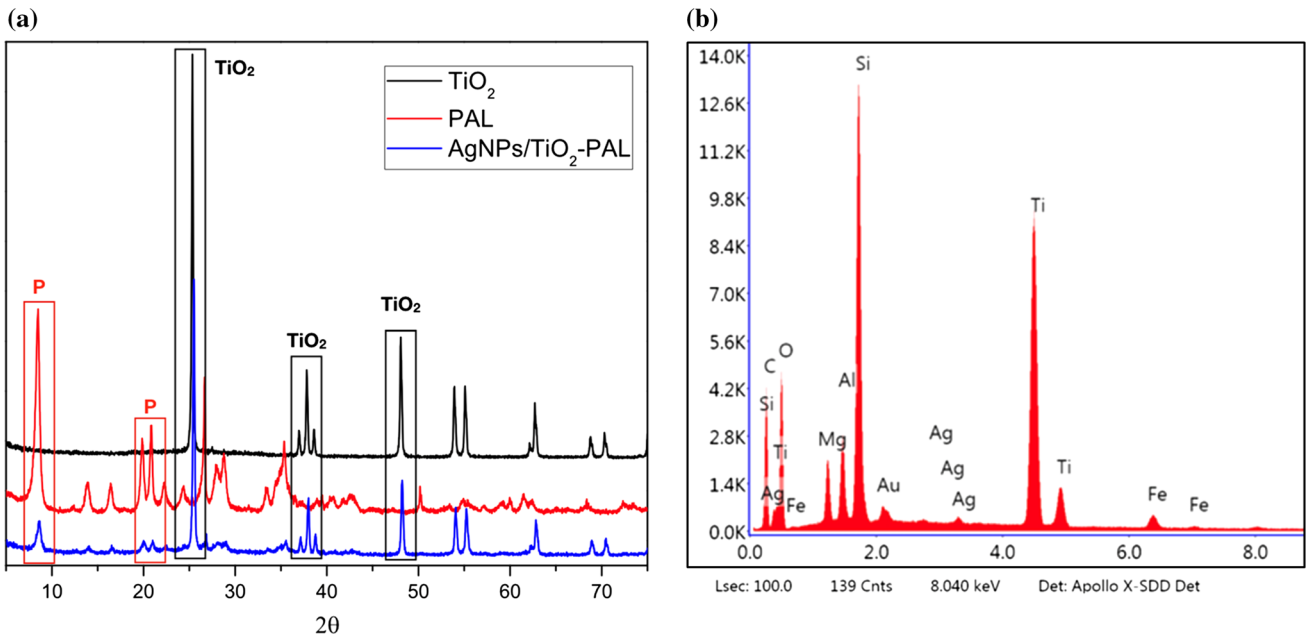

Fig. 2 **a** AgNPs/TiO_2-PAL catalyst diffractogram and **b** EDS graph of AgNPs/TiO_2-PAL catalyst

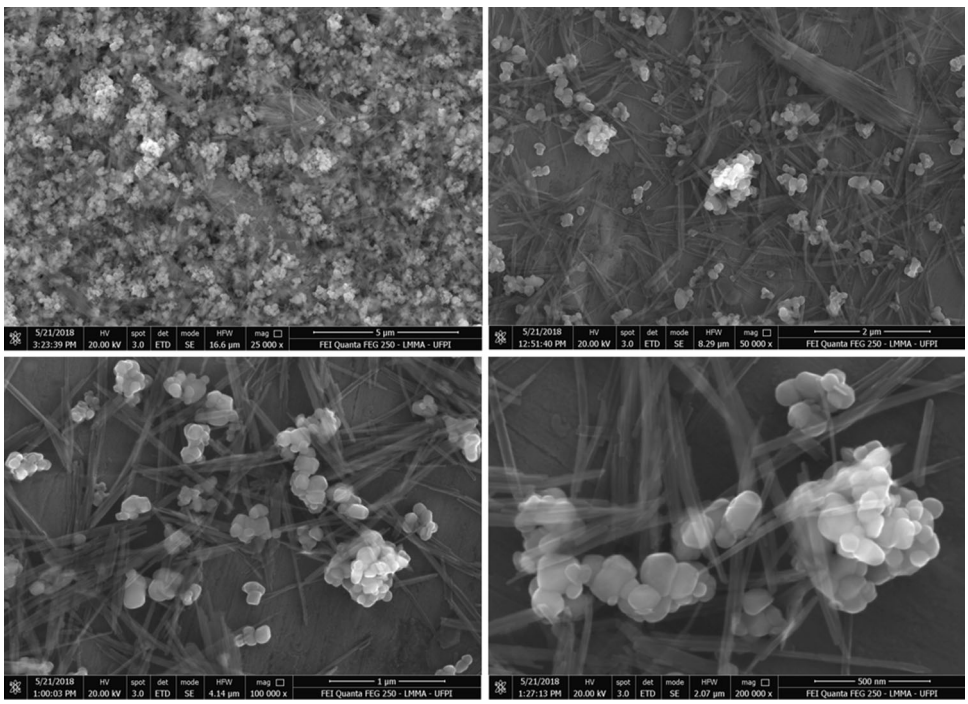

Fig. 3 SEM images of AgNPs/TiO_2-PAL

morphology of palygorskite (Guo et al. 2014). Many AgNPs/TiO_2 particles were distributed on the surface of PAL fibers. The hydroxyl group on the surface of crystal structure of PAL was lost during the calcination process thus helping in stabilization of TiO_2 on the PAL to form stable Ti–O–Si bond (Ma et al. 2017). This structure enhanced the photocatalytic properties by reducing the grain size of TiO_2 in the catalysts.

Despite all merits, TiO_2 has some limitations which tend to hamper its practical application, for example, due to its wide band gap, it is active only in the ultra-violet region of solar spectrum which comprises only 4% of the total solar spectrum, it has low adsorption capability due to the relatively low surface area and porosity, it has high aggregation tendency and it tends to form a colloidal suspension in

an aqueous medium which makes its recovery difficult (Mishra et al. 2018).

The modification of the surface of the TiO_2 from the addition of silver nanoparticles comes as an alternative to enhance the activity of TiO_2 towards the visible region of the solar spectrum (Kaur and Pal 2015). And the support of this composite in the palygorskite clay is the solution to the problems de low surface area and porosity, besides solving the problem of high aggregation tendency and it tends to form a colloidal suspension in an aqueous medium, facilitating catalyst recovery (Mishra et al. 2018).

Development of the analytical method for recognition of antioxidant activity

The reactive oxygen species generated by the photocatalytic oxidation of water using TiO_2 are the hydroxyl radical ($HO^{\cdot}$), superoxide anion ($O_2^{\cdot -}$) and singlet oxygen ($^1O_2$) (Rui-Jie et al. 2016; Nagarajan et al. 2017). These species are biologically present in vivo, playing important roles in various biochemical reactions. The superoxide anion ($O_2^{\cdot -}$) is continuously generated in the electron transport chain in the mitochondria, by the action of enzymes such as xanthine oxidase and NADPH oxidase, or by the monoelectronic reduction of O_2. In relation to other reactive species, the $O_2^{\cdot -}$ has a relatively long half-life, which allows diffusion within the cell, thereby increasing the number of potential targets (Carocho et al. 2018). The $HO^{\cdot}$ radical is the most reactive and most damaging radical known and for which, once formed, the human organism has no defense mechanism, although it has a short half-life (approximately 10^{-9} s), reacts rapidly and without selectivity to a series of endobiotics, causing DNA modification, lipid peroxidation, protein damage, and enzymatic inactivation (Mozafari et al. 2006). The $^1O_2$ consists of the electronically excited state of oxygen, produced by photochemical reactions or other radiations, it reacts with a large number of biological molecules, including DNA, proteins and lipids, and although it's not a free radical, it causes the formation of other toxic radicals, since it is one of the most active intermediates involved in biochemical reactions (Costa et al. 2007).

A general process for photocatalysis initiates from the photoexcitation of TiO_2 with an energy greater than its band gap (Eg) of 3.2 eV (Wei et al. 2017), resulting in the formation of active electron–hole pairs (e^-/h^+) (Wei et al. 2017). In the presence of electron donors and acceptors in solution, the recombination reaction between the electron and the hole can be avoided by redox reactions. In the photolysis of TiO_2 in water, the solvating nanoparticles of the water molecules and the dissolved O_2 can react with both the hole and the electron, respectively, to generate $HO^{\cdot}$ and $O_2^{\cdot -}$, these in turn react and form oxygen singlet $^1O_2$ (Rui-Jie et al. 2016; Nagarajan et al. 2017).

$$TiO_2 + h\nu \rightarrow e^-_{CB} + h^+_{VB} \quad (2)$$

$$H_2O + h^+_{VB} \rightarrow H^+ + OH^{\cdot} \quad (3)$$

$$2OH^-_{ads} + h^+_{VB} \rightarrow OH^- + OH^{\cdot} \quad (4)$$

$$e^-_{CB} + O_2 \rightarrow O_2^{\cdot -} \quad (5)$$

$$2O_2^{\cdot -} + 2H_2O \rightarrow 2OH^{\cdot} + 2OH^- + O_2 \quad (6)$$

$$\text{dye} + OH^{\cdot} \rightarrow \text{degradation products} + CO_2 + H_2O \quad (7)$$

$$\text{dye} + h^+_{VB} \rightarrow \text{oxidation products} \quad (8)$$

$$\text{dye} + e^-_{CB} \rightarrow \text{reduction products} \quad (9)$$

The adequate linearity of the method was verified by the linear regression analysis of the antioxidant concentration evaluated versus the discoloration of the AY73 for each concentration (Fig. 4) and it could be verified an antioxidant capacity of gallic acid on the AgNPs/TiO_2-PAL system in concentration-dependent manner.

Considering the equations described in Fig. 4 it is possible to find the antioxidant concentration necessary to protect the dye from 50% of the AY73 discoloration (IC_{50}) in the presence of the catalysts and UV light. The IC_{50} value obtained for gallic acid using the catalyst AgNPs/TiO_2-PAL was 12 ± 2.5 μg mL^{-1}, while, using the catalyst TiO_2 P25 Degussa was 50 ± 4.3 μg mL^{-1}.

Masaki et al. (1994) evaluated the ability of inhibiting reactive species such as superoxide anion, hydroxyl radicals and singlet oxygen for antioxidants known as gallic acid, propyl gallate and ascorbic acid. Gallic acid showed better results for most reactive species studied, with IC_{50}

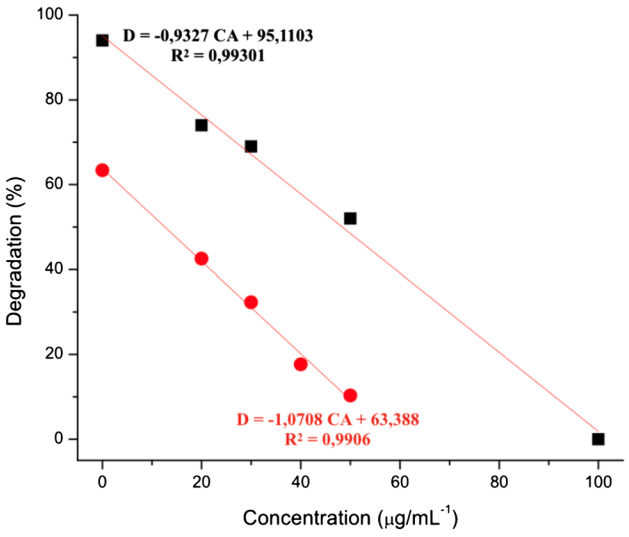

Fig. 4 Gallic acid analytical curves. CA is the concentration of antioxidant evaluated; D is the discoloration of the AY73. *Black filled square* TiO_2 P25 Degussa, *Red filled circle* AgNPs/TiO_2-PAL

values 11.86 ± 0.79 μg mL^{-1} for singlet oxygen ($^1O_2$), 0.187 ± 0.03 μg mL^{-1} for superoxide anion and 13.33 ± 1.91 μg mL^{-1} for hydroxyl radicals.

Lo Scalzo (2010) evaluated the antioxidant capacity of gallic acid to eliminate reactive species $O_2^{\cdot-}$ and $HO^{\cdot}$, the study was performed by electronic paramagnetic resonance. The value of the minimum inhibitory concentrations of gallic acid found by the $O_2^{\cdot-}$ was 3.9 mM, while for $HO^{\cdot}$ was 781.5 mM. Thus, the author concluded that the potential of gallic acid to inhibit reactive species $O_2^{\cdot-}$ and $HO^{\cdot}$ is very distinct, a very low concentration of antioxidant is required to inhibit $O_2^{\cdot-}$ compared to the concentration required to inhibit $HO^{\cdot}$.

Chisté et al. (2012) found IC_{50} values for gallic acid of 13 ± 2 μg mL^{-1} for neutralization of $O_2^{\cdot-}$ and 1 ± 0.06 μg mL^{-1} for $^1O_2$, but the IC_{50} for $HO^{\cdot}$ was not evaluated. Ribeiro et al. (2014) evaluated the in vitro elimination capacity of extracts of the *Psidium cattleianum* fruit against reactive oxygen species (ROS) and reactive nitrogen species (RNS), and compared the results obtained with antioxidants known as gallic acid, ascorbic acid and quercetin. Gallic acid showed IC_{50} of 1.6 ± 0.10 μg mL^{-1} for $^1O_2$ and 3.9 ± 0.10 μg mL^{-1} for $O_2^{\cdot-}$.

Considering the above, it is possible to notice that the great majority of the studies evaluate the antioxidant capacity of the compounds/extracts/materials and antioxidants considered as gold standard for isolated reactive species, being an interesting way to understand the mechanism of action of antioxidants. However, in studies using in vivo systems, the reactive species are produced cascaded and do not react in isolation. Therefore, in the method developed in the present study, IC_{50} of gallic acid 12 ± 2.5 μg mL^{-1} was used using the AgNPs/TiO_2-PAL catalyst and 50 ± 4.3 μg mL^{-1}, using the TiO_2 P25 catalyst, to eliminate three reactive species $O_2^{\cdot-}$, $HO^{\cdot}$ and $^1O_2$ produced, where $O_2^{\cdot-}$, $HO^{\cdot}$ are produced simultaneously and depart from these as $^1O_2$, which occur naturally and constantly in the biochemical reactions of the in vivo systems (Rui-Jie et al. 2016; Nagarajan et al. 2017).

UV–vis spectra of the AY73

It is considered that the reactive species generated by the TiO_2 catalyst during the photocatalysis of the water are responsible for discoloration of the AY73. However, in the presence of a compound with antioxidant potential, such as gallic acid, discoloration could potentially be minimized, suggesting that this system could be used for the development of a simple, fast and low-cost methodology to qualitatively and quantitatively determine the antioxidant capacity of natural and synthetic compounds of new materials.

Thus, the dye residue AY73 in the aqueous solution after the antioxidant activity assays were evaluated by UV–vis spectroscopy. The acid yellow dye 73 showed maximum absorption band at wavelength 490 nm, in addition to smaller bands at wavelengths 238, 285 and 324 nm.

The spectrum of AY73 using the AgNPs/TiO_2-PAL catalyst, Fig. 5a, and the catalyst TiO_2 P25 Degussa, Fig. 5b, shows that the intensity of the peaks at 490 nm decreases gradually during UV irradiation, resulting in discoloration of the solutions. The near-perfect disappearance of the band at 490 nm reveals that AY73 is eliminated after about 60 min in the systems consisting of aqueous solution of the dye and catalyst, without addition of antioxidant. No new absorption peak appeared in the visible or UV regions. After 60 min of exposure to UV light in the presence of the AgNPs/TiO_2-PAL catalyst the discoloration was 80% and in the presence of the catalyst TiO_2 P25 Degussa was 86%.

By adding the gallic acid antioxidant to the system it is observed in the spectrum of AY73 using the AgNPs/TiO_2-PAL catalyst, Fig. 5c, and the catalyst TiO_2 P25 Degussa, Fig. 5d, that the intensity of the peaks at 490 nm (λmax) suffers only a reduction, which does not result in the total discoloration of the solutions, indicating that this compound with antioxidant potential recognized in the literature scavenges the reactive oxygen species of the reaction medium, significantly reducing their reaction with the dye.

Pathway of reactive oxygen species (ROS)

The best way to understand the role of each reactive species in the antioxidant capacity assays is to try to retard the recombination of photogenerated holes and electrons on the surface of the catalyst, that is, to fill the holes of the valence band with the electrons of some type of reducer (Alrobayi et al. 2015).

In the present study, scavengers were used, as methanol to remove radicals $HO^{\cdot}$ (Li and Hu 2016), diphenylamine as $O_2^{\cdot-}$ remover (Alrobayi et al. 2015) and furfural alcohol as $^1O_2$ remover (Li and Hu 2016). The results of the photocatalytic discoloration of AY73 in the antioxidant capacity assays in system with suppressors can be seen in Fig. 6a.

By adding diphenylamine (suppressor of $O_2^{\cdot-}$), methanol ($HO^{\cdot}$ suppressor), furfuryl alcohol (suppressor of $^1O_2$) and EDTA disodium salt (h^+ suppressor) to the system composed of aqueous solution of dye and AgNPs/TiO_2-PAL catalyst, a significant reduction in the discoloration of the AY73 was achieved.

Li et al. (2013), obtained similar results regarding the order of importance of the reactive species in the methyl orange dye degradation using the TiO_2 catalyst and adding $AgNO_3$ in the solution. The authors describe that by

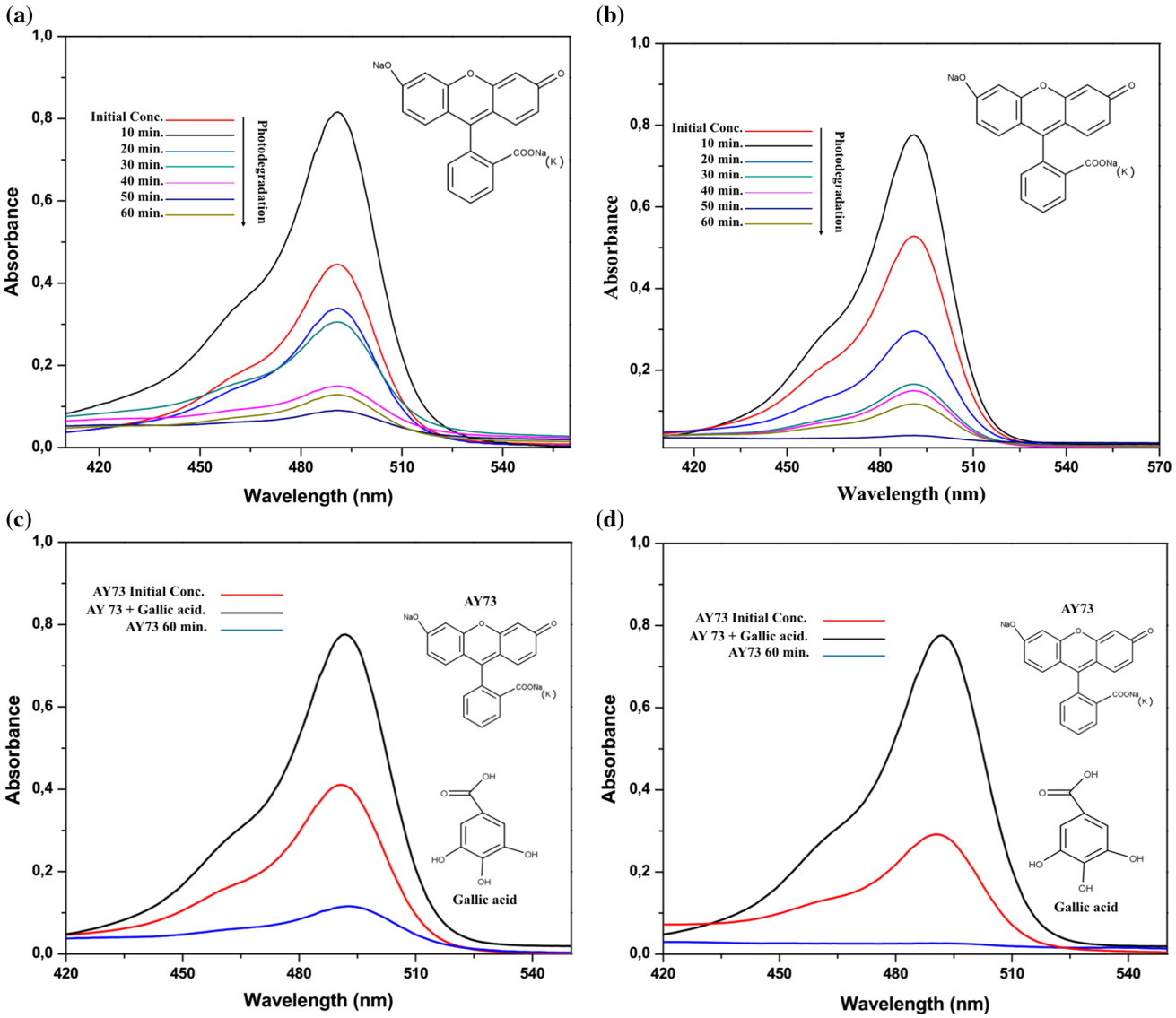

Fig. 5 UV-vis spectrum of the AY73: **a** AgNPs/TiO_2-PAL catalyst in the absence of antioxidant; **b** TiO_2 P25 in the absence of antioxidant; **c** AgNPs/TiO_2-PAL catalyst in the presence of antioxidant and **d** TiO_2 P25 in the presence of antioxidant

combining the important role of $HO^{\cdot}$ radicals with the almost insignificant role of holes in dye degradation, it is possible to deduce that there is another source of $HO^{\cdot}$ radical generation in the system besides the generation through the holes. When comparing this deduction with the fact that suppressing $O_2^{\cdot-}$ in the reactions in this work caused a great impact in the degradation of the dye AY73, it is possible to conclude that $O_2^{\cdot-}$ can be another source of generation of radicals $HO^{\cdot}$.

Liu et al. (2007), synthesized a photocatalyst composed of TiO_2 and silver, supported on montmorillonite (Ag-TiO_2/MMT) and applied to the photodegradation of the methylene blue dye (MB), among Ag-TiO_2, MMTNTiO_2, MMTNTiO_2 (P25) and Ag-TiO_2/MMT, the Ag-TiO_2/MMT exhibited the highest photooxidation activity because of its larger specific surface caused by pillaring and loading of silver for improving its light absorption.

So, the transfer of electrons to metal deposits in TiO_2, results in the metal becoming negatively charged. In air-equilibrated systems, Ag deposits on the TiO_2 surface enhance photoactivity by accelerating the transfer of electrons to dissolved oxygen molecules. Therefore, the superoxide anion radical is formed as a result of oxygen reduction by transfer of trapped electrons from Ag metal to oxygen (Behnajady et al. 2007).

The oxidation of AY73 by photocatalysis in the system with AgNPs/TiO_2-PAL was carried out mainly by the participation of $O_2^{\cdot-}$, $HO^{\cdot}$ and $^1O_2$ species, in this order of importance. In addition, it is possible to verify that the contribution of the holes occurred on a smaller scale.

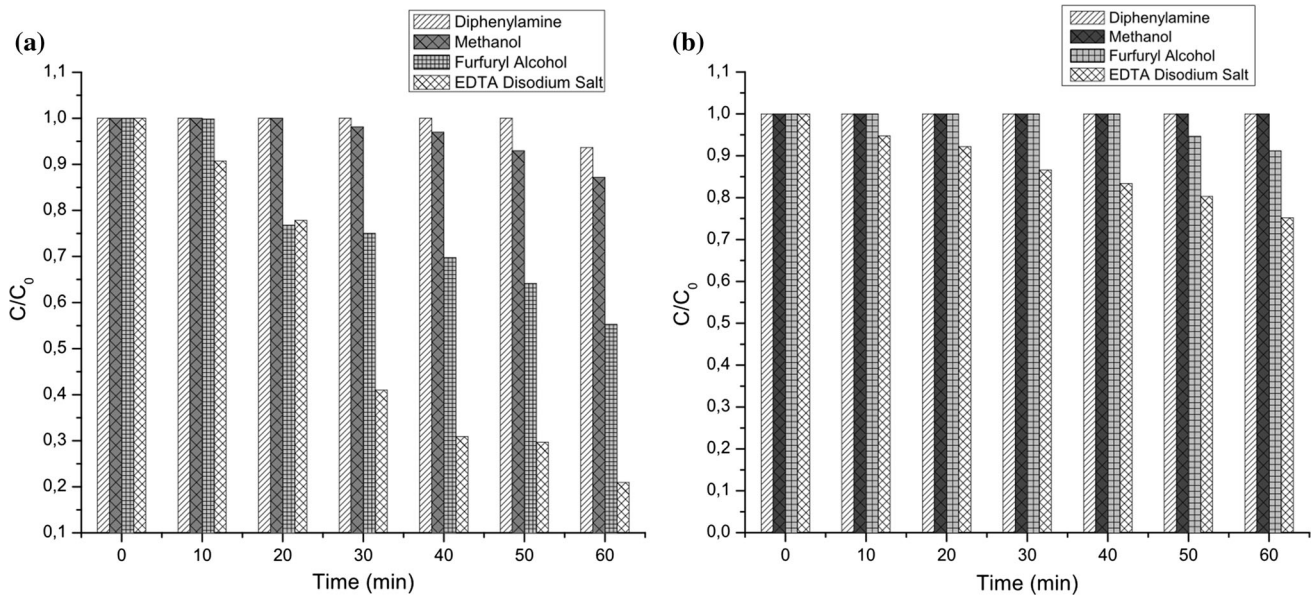

Fig. 6 **a** Photocatalytic discoloration of AY73 in the antioxidant capacity assays by adding the suppressors and **b** Photocatalytic discoloration of AY73 in the antioxidant capacity assays by adding the suppressors and antioxidant

Adding the gallic acid antioxidant to these systems, it is seen that the AY73 protection efficiency increases with the addition of all suppressors, Fig. 6b. There is a significant reduction, in the AY73 discoloration with the addition of furfuryl alcohol and EDTA Disodium (h^+ suppressor). On the other hand, a protection of almost 100% of the color of the dye is observed in both systems with the addition of diphenylamine (suppressor of radicals $O_2^{\cdot-}$) and methanol ($HO^{\cdot}$ suppressor).

Conclusion

A catalyst constituted of TiO_2, palygorskite and silver nanoparticles (AgNPs/TiO_2-PAL), was synthesized and applied to the development of a method of recognizing the antioxidant capacity. The most favorable results for the protection of the dye by the antioxidant was observed when using the synthesized catalyst that demonstrating greater sensitivity to the system presenting a lower IC_{50} for protection of the dye than the commercial catalyst. The additional study of the ROS contribution indicates that $O_2^{\cdot-}$ and $HO^{\cdot}$ are responsible for the greater discoloration of AY73 using the AgNPs/TiO_2-PAL catalyst, while $^1O_2$ and $HO^{\cdot}$ are responsible for the greater discoloration of AY73 using the TiO_2 P25 Degussa catalyst.

In this way it can be verified that the catalyst was synthesized efficiently and demonstrated excellent applicability to the developed method, which presents potential to be used in industrial and universities laboratories to investigate antioxidant activity in natural/synthetic compounds and new materials with applications for food, cosmetics and pharmaceutical industries.

References

Abou El-Nour KMM, Eftaiha A, Al-Warthan A, Ammar RAA (2010) Synthesis and applications of silver nanoparticles. Arab J Chem 3(3):135–140. https://doi.org/10.1016/j.arabjc.2010.04.008

Agnihotri S, Mukherji S, Mukherji S (2014) Size-controlled silver nanoparticles synthesized over the range 5–100 nm using the same protocol and their antibacterial efficacy. RSC Adv 4:3974–3983. https://doi.org/10.1039/C3RA44507K

Alrobayi EM, Algubili AM, Aljeboree AM, Alkaim AF, Hussein FH (2015) Investigation of photocatalytic removal and photonic efficiency of maxilon blue dye GRL in the presence of TiO_2 nanoparticles. Part Sci Technol. https://doi.org/10.1080/02726351.2015.1120836

Behnajady MA, Modirshahla N, Shokri M, Rad B (2007) Enhancement of photocatalytic activity of TiO_2 nanoparticles by silver doping: photo deposition versus liquid impregnation methods. Glob Nest J 10(1):1–7

Carocho M, Morales P, Ferreira ICFR (2018) Antioxidants: reviewing the chemistry, food applications, legislation and role as preservatives. Trends Food Sci Technol 71:107–120. https://doi.org/10.1016/j.tifs.2017.11.008

Chen D, Du Y, Zhu H, Deng Y (2014) Synthesis and characterization of a micro fibrous TiO_2–CdS/palygorskite nanostructured material with enhanced visible light photocatalytic activity. Appl Clay Sci 87:285–291. https://doi.org/10.1016/j.clay.2013.11.031

Chisté RC, Freitas M, Mercadante AZ, Fernandes E (2012) The potential of extracts of *Caryocar villosum* pulp to scavenge reactive oxygen and nitrogen species. Food Chem 135:1740–1749. https://doi.org/10.1016/j.foodchem.2012.06

Costa D, Fernandes E, Santos JLM, Pinto DCGA, Silva AMS, Lima JLFC (2007) New noncellular fluorescence microplate screening assay for scavenging activity against singlet oxygen. Anal Bio

Anal Chem 387:2071–2081. https://doi.org/10.1007/s00216-006-0998-9

Erel O (2004) A novel automated direct measurement method for total antioxidant capacity using a new generation, more stable ABTS radical cation. Clin Biochem 37:277–285. https://doi.org/10.1016/j.clinbiochem.2003.11.015

Ge Q, Ge P, Jiang D, Du N, Chen J, Yuan L, Yu H, Xu X, Wu M, Zhang W, Zhou G (2018) A novel and simple cell-based electrochemical biosensor for evaluating the antioxidant capacity of *Lactobacillus plantarum* strains isolated from Chinese dry-cured ham. Biosens Bioelectron 99:555–563. https://doi.org/10.1016/j.bios.2017.08.037

Guo X, Qiu F, Dong K, Rong X, He K, Xu J, Yang D (2014) Preparation and application of copolymer modified with the palygorskite as inhibitor for calcium carbonate scale. Appl Clay Sci 99:187–193. https://doi.org/10.1016/j.clay.2014.06.031

Hidalgo MC, Maicu M, Navio JA, Colon G (2010) Effect of sulfate pretreatment on gold-modified TiO_2 for photocatalytic applications. J Phys Chem 113:12840–12847. https://doi.org/10.1021/jp903432p

Kaur R, Pal B (2015) Plasmonic coinage metal-TiO_2 hybrid nanocatalysts for highly efficient photocatalytic oxidation under sunlight irradiation. New J Chem 39(8):5966–5976. https://doi.org/10.1039/C5NJ00450K

Kumar S, Sharma S, Vasudeva N (2017) Review on antioxidants and evaluation procedures. Chin J Integr Med. https://doi.org/10.1007/s11655-017-2414-z

Lee DS, Chen YW (2014) Nano Ag/TiO_2 catalyst prepared by chemical deposition and its photocatalytic activity. J Taiwan Inst Chem Eng 42(2):705–712. https://doi.org/10.1016/j.jtice.2013.07.007

Li S, Hu J (2016) Photolytic and photocatalytic degradation of tetracycline: effect of humic acid on degradation kinetics and mechanisms. J Hazard Mater 318:134–144. https://doi.org/10.1016/j.jhazmat.2016.05.100

Li W, Li D, Wang J, Shao Y, You J, Teng F (2013) Exploration of the active species in the photocatalytic degradation of methyl orange under UV light irradiation. J Mol Catal A Chem 380:10–17. https://doi.org/10.1016/j.molcata.2013.09.001

Liu J, Li X, Zuo S, Yu Y (2007) Preparation and photocatalytic activity of silver and TiO_2nanoparticles/montmorillonite composites. Appl Clay Sci 37:275–280. https://doi.org/10.1016/j.clay.2007.01.008

Lo Scalzo R (2010) Measurement of free radical scavenging activity of gallic acid and unusual antioxidants as sugars and hydroxy acids. Electron J Environ Agric Food Chem 9(8):1360–1371

López-Alarcón C, Denicola A (2013) Evaluating the antioxidant capacity of natural products: a review on chemical and cellular-based assays. Anal Chim Acta 763:1–10. https://doi.org/10.1016/j.aca.2012.11.051

Ma J, Zhu C, Xu Y, Lu J, Huang L, Yang Z (2017) Photocatalytic degradation of gaseous benzene with $H_3PW_{12}O_{40}$/TiO_2/palygorskite composite catalyst. J Saudi Chem Soc 21(2):132–142. https://doi.org/10.1016/j.jscs.2015.02.001

Masaki H, Atsumi T, Sakurai H (1994) Hamamelitannin as a new potent active oxygen scavenger. Phytochemistry 37(2):337–343. https://doi.org/10.1016/0031-9422(94)85057-7

Mecha AC, Onyango MS, Ochieng A, Jamil TS, Fourie CJ, Momba MNB (2016) UV and solar light photocatalytic removal of organic contaminants in municipal wastewater. Sep Sci Technol 51(10):1765–1778. https://doi.org/10.1080/01496395.2016.1178290

Mishra A, Mehta A, Basu S (2018) Clay supported TiO_2 nanoparticles for photocatalytic degradation of environmental pollutants: a review. J Environ Chem Eng 6(5):6088–6107. https://doi.org/10.1016/j.jece.2018.09.029

Mozafari MR, Flanagan J, Martia-Merino L, Awati A, Omri A, Suntres ZE, Singh H (2006) Recent trends in the lipid-based nanoencapsulation of antioxidants and their role in foods. J Sci Food Agric 86(13):2038–2045. https://doi.org/10.1002/jsfa.2576

Nagarajan S, Skillena NC, Fina F, Zhang G, Randorn C, Lawton LA, Irvine JTS, Robertson PKJ (2017) Comparative assessment of visible light and UV active photocatalysts by hydroxyl radical quantification. J Photochem Photobiol A Chem 334:13–19. https://doi.org/10.1016/j.jphotochem.2016.10.034

Niki E (2010) Assessment of antioxidant capacity in vitro and in vivo. Free Radic Biol Med 49:503–515. https://doi.org/10.1016/j.freeradbiomed.2010.04.016

Ribeiro AB, Chisté RC, Freitas M, da Silva AF, Visentainer JV, Fernandes E (2014) *Psidium cattleianum* fruit extracts are efficient in vitro scavengers of physiologically relevant reactive oxygen and nitrogen species. Food Chem 165:140–148. https://doi.org/10.1016/j.foodchem.2014.05.079

Rui-Jie J, Qiang Z, Ji-Feng L, Mohamad H, Girault HH (2016) Antioxidant assay based on quenching of photocatalytically generated reactive oxygen species. Chin J Anal Chem 44(8):1257–1262. https://doi.org/10.1016/S1872-2040(16)60950-7

Samya E, Fatma M, Marwa S, Osama AF (2014) Synthesis, characterization and application of TiO_2 nanopowders as special paper coating pigment. Appl Nanosci 4:305–313. https://doi.org/10.1007/s13204-013-0196-y

Santana H, Zaia DAM (2006) Preparação e caracterização de substratos SERS ativos: um estudo da adsorção do cristal violeta sobre nanopartículas de prata. Quím Nova 29(2):194–199

Soberanis-Monforte GA, Gordillo-Rubio JL, González-Chi PI (2015) Influence of chemically treated palygorskite over the rheological behavior of polypropylene nanocomposites. Ing Invest Tecnol 16:491–501. https://doi.org/10.1016/j.riit.2015.09.002

Tian C, Zhang Q, Wu A, Jiang M, Liang Z, Jiang B, Fu H (2012) Cost-effective large-scale synthesis of ZnO photocatalyst with excellent performance for dye photodegradation. Chem Commun 48:2858–2860. https://doi.org/10.1039/C2CC16434E

Verma A, Prakash NT, Toor AP (2014) An efficient TiO_2 coated immobilized system for the degradation studies of herbicide isoproturon: durability studies. Chemosphere 109:7–13. https://doi.org/10.1016/j.chemosphere.2014.02.051

Wei M, Peng XL, Liu QS, Li F, Yao MM (2017) Nanocrystalline TiO_2 composite films for the photodegradation of formaldehyde and oxytetracycline under visible light irradiation. Molecules 22(6):950. https://doi.org/10.3390/molecules22060950

Zhang Lili, Liu J, Tang C, Lv J, Zhong H, Zhao Y, Wang Y (2011) Palygorskite and SnO_2–TiO_2 for the photodegradation of phenol. Appl Clay Sci 51:68–73. https://doi.org/10.1016/j.clay.2010.11.003